

Holmium growth on Si(001): Surface reconstructions and nanowire formation

C. Ohbuchi and J. Nogami

Department of Physics and Astronomy, Department of Chemical Engineering and Materials Science, and the Center for Fundamental Materials Research, Michigan State University, East Lansing, Michigan 48824

(Received 17 June 2002; published 30 October 2002)

Holmium deposition on the Si(001) surface at elevated temperature results in the formation of Ho silicide islands coexisting with a Ho reconstructed substrate surface. At metal coverages below a monolayer, most of the islands are highly elongated nanowires. Structural details of both the reconstructions and the nanowires derived from scanning tunneling microscope data are presented. In addition, scanning tunneling spectroscopy shows that the nanowires are more metallic than either the reconstructed surface, or large silicide islands.

DOI: 10.1103/PhysRevB.66.165323

PACS number(s): 68.37.Ef, 61.46.+w, 68.55.-a

I. INTRODUCTION

Epitaxial rare-earth (RE) silicides grown on silicon have attracted particular interest because of the tunable lattice mismatch between the silicide and silicon.¹ In the study of RE silicides grown on Si(001), it has been reported that several RE silicides can form nanowires. Preinesberger *et al.* first showed that Dy on Si(001) forms nanowires under certain conditions,² and then Chen *et al.* demonstrated that nanowires can also be grown in the case of ErSi₂ on Si(001).³ Holmium is another RE metal which can form nanowires on Si(001).⁴ This nanowire formation is ascribed to good lattice match in one direction and bad lattice match in the perpendicular direction.^{3,4}

Although a few structural studies of Ho on Si(111) have been done,^{5,6} there has been no investigation in Ho on Si(001) surface yet. In this work we present a scanning tunneling microscopy (STM) and scanning tunneling spectroscopy (STS) study of Ho growth on Si(001).

II. EXPERIMENTAL METHODS

All experiments were performed in an ultra high vacuum (UHV) system with a base pressure of $<2 \times 10^{-10}$ Torr. The chamber was equipped with an STM, a four-grid low energy electron diffraction (LEED) optics, and facilities for sample heating and metal deposition. The Si(001) samples were *p*-type wafers (2.6 Ω cm), chemically cleaned, and then outgassed by heating to 975 °C. After outgassing, they were flashed briefly at 1160 °C to remove surface oxide, and held at 975 °C for 10 min, and then cooled slowly to room temperature (RT). The temperatures of the samples were measured using an optical pyrometer. Holmium was evaporated from a tungsten wire basket, and the evaporation rate was calibrated by a quartz-crystal thickness monitor. Typical evaporation rates were 0.05–0.09 monolayers (ML) per minute [1 ML = 6.78×10^{14} cm⁻²] and total coverages studied were between 0.06–0.9 ML. The chamber pressure remained below 1×10^{-8} Torr during evaporation, and immediately recovered to below 5×10^{-10} Torr after the metal source was turned off. All growth was done at a substrate temperature of 600 °C. All STM imaging and LEED observation were done at RT.

III. RESULTS AND DISCUSSION**A. Coverage dependence**

Figure 1 shows the coverage dependence of Ho growth on Si(001) at 600 °C. The horizontal axis is the metal coverage in monolayers (ML), and both LEED pattern and topography are shown. Black circles are the metal coverages at which experiments were done. There are roughly two types of topographies, both of which are comprised of a two-dimensional (2D) reconstructed substrate, coexisting with three dimensional (3D) silicide islands. The LEED patterns reflect the 2D ordered surface. For low metal coverage, $\Theta \leq 0.4$ ML, the islands are highly elongated nanowires with typical width 1.1–7.3 nm, height 0.2–1.2 nm, and lengths 100–500 nm [Fig. 2(a)]. As the coverage increases, 3D compact silicide islands are found of varying shape [Fig. 2(b)]. Nanowires and 3D islands coexist at coverages above 0.4 ML. A 2×4 phase dominates the 2D reconstructed surface structure at most of the coverages shown in Fig. 1 although clean Si 2×1 dimer rows are observed in places below 0.18 ML. In addition, a 2×7 phase appears in the 0.4–0.55 ML coverage regime, and it coexists with the 2×4 phase.

The percentage of the 2D surface covered with Ho in either the 2×4 or the 2×7 phase is not monotonic with coverage as shown in Fig. 3. At lowest coverage, 0.06 ML, there is only 2×4 structure and bare Si on the 2D surface. As the coverage is increased, most of the 2D surface is covered by the 2×4 structure, and both the density and the average height of nanowires increase. When 3D islands appear, the percentage of the 2D surface covered by 2×4 de-

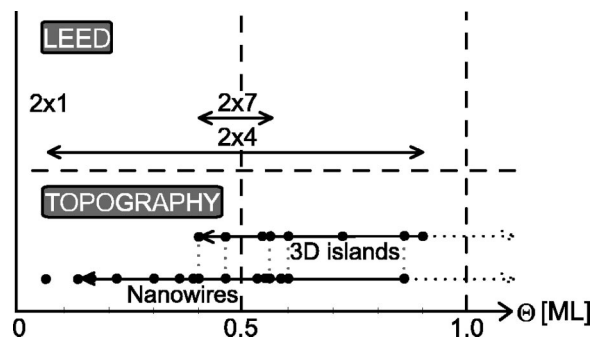


FIG. 1. Coverage dependence of LEED patterns and topography for Ho growth on Si(001) at 600 °C.

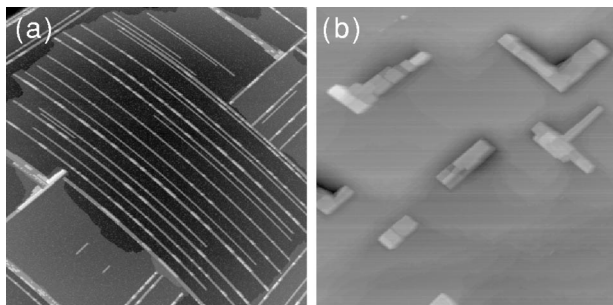


FIG. 2. Two $400 \times 400 \text{ nm}^2$ images of Ho nanowires and 3D islands. (a) Nanowires formed by 0.36 ML of Ho. Each nanowire grows on a single terrace. (b) As the coverage is increased (0.90 ML), 3D compact silicide islands are found.

creases and bare Si substrate reappears. From mass conservation, Ho atoms moved from the 2D surface to the 3D islands. This fact implies 3D silicide islands are preferable to either a Ho reconstructed substrate, or the elongated nanowires in terms of accommodation of Ho. The initial stage of nanowire growth can be described as Stranski-Krastanov. However, the reappearance of bare Si once 3D islands are formed shows that the growth mode changes to Volmer Weber at higher coverage.

B. Nanowires and 3D islands

As seen in Fig. 2(a), every nanowire grows on a single atomic terrace, and runs along a $\langle 1\bar{1}0 \rangle$ type direction. Each nanowire usually terminates at a step edge or at a perpendicular nanowire, but perpendicular nanowires are on different terraces and do not cross. At higher coverages, rectangular islands can nucleate at the intersection of nanowires. The nanowires in Fig. 2(a) are comparatively long as the step density on this substrate is low. On substrates with higher step density, steps can flow to accommodate nanowires, as shown in Fig. 4(a). In this image, the steps curve to follow the nanowires so that each remains on a single terrace. Nevertheless, there is some limit to the number of steps that can flow to accommodate a nanowire, and so nanowire length is still limited by step density.

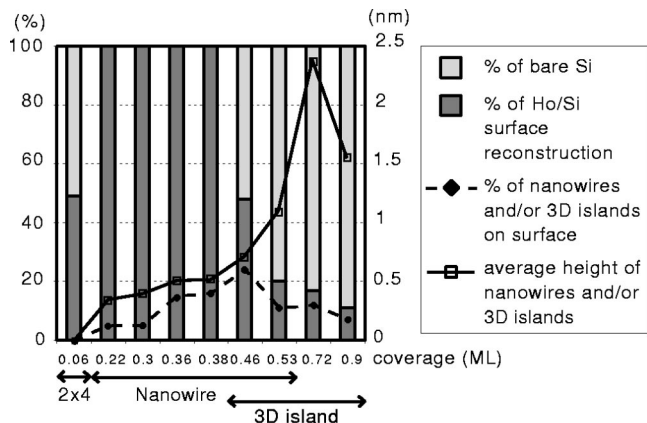


FIG. 3. Relationship between coverage and the percentage of surface covered with Ho surface reconstruction, nanowires, and 3D islands.

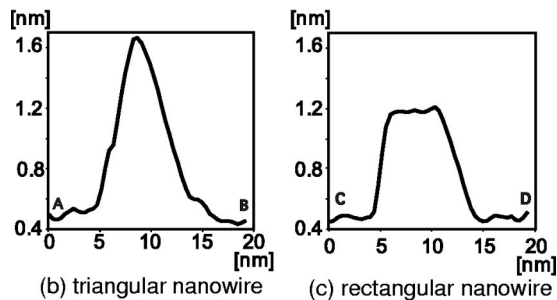
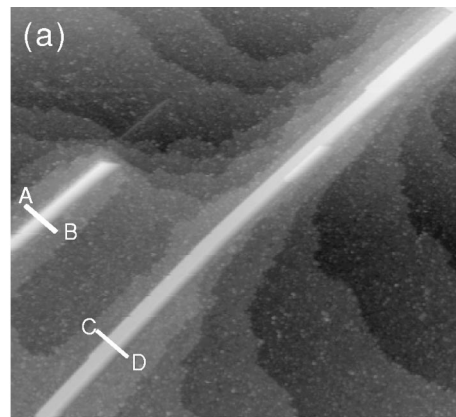


FIG. 4. (a) Triangular (left) and rectangular (right) nanowires at 0.3 ML ($200 \times 200 \text{ nm}^2$). Steps on the substrate flow to accommodate the nanowires. Lines A-B and C-D show the locations of the cross sections shown in (b) and (c).

As shown in Fig. 4(a), there are two distinct nanowire morphologies: one is triangular in cross section, and the other is rectangular. Figures 4(b) and 4(c) are cross-sectional profiles of these nanowires. At 0.2–0.3 ML, both types of nanowires are seen at equal probability. As the coverage increases up to 0.4 ML, rectangular nanowires are more often observed and at the same time nanowires tend to form parallel bundles as shown in Fig. 5(a). While the narrow nanowires at the edges of bundles are mostly triangular in cross section, those in the middle of the bundles are certainly rectangular.

The structure of the rectangular nanowires can be understood in terms of the bulk silicide $\text{HoSi}_{1.7}$, which has a hexagonal AlB_2 type structure, with the $[0001]$ axis parallel to

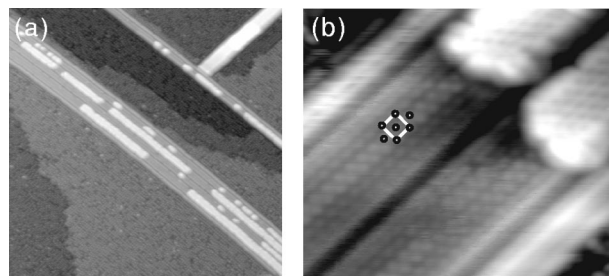


FIG. 5. (a) Bundled nanowires with second layer growth at 0.36 ML ($90 \times 90 \text{ nm}^2$). (b) Atomic resolution on bundled nanowires ($12 \times 14 \text{ nm}^2$). A single $c(2 \times 2)$ unit cell is marked with a white square.

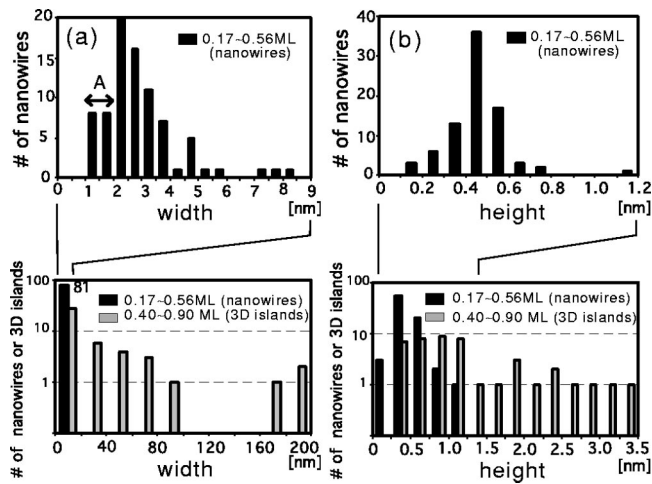


FIG. 6. The distributions of the width (a) and the height (b) of single nanowires and 3D islands.

the surface, and the $[1\bar{1}20]$ direction along the long axis of the nanowire.^{3,4} Atomic resolution on the top surface of rectangular nanowires show $c(2 \times 2)$ periodicity [Fig. 5(b)]. The same periodicity is seen on the surface of second layer nanowire growth. The height of the second layer nanowire is always 0.33 nm which corresponds to 1 bulk HoSi_2 unit cell height.⁴ This height includes one metal layer and two Si layers. The apparent height of the first nanowire silicide layer varies because the electronic properties of the nanowire and substrate surface are different. The structure of the triangular cross section nanowires is not clear from the STM data, but it is likely that it has the same epitaxial characteristic of the rectangular nanowire with the $[1\bar{1}20]$ direction lying along the long axis. It is possible that these triangular wires are simply a minimal width rectangular wire with perhaps a different step edge structure.

When the widths and the heights of silicide islands are measured, it is clear that the 3D compact silicide islands have widely varying dimensions whereas those of nanowires are restricted to narrow ranges. Figures 6(a) and 6(b) are the distributions of the width and the height of single nanowires and compact silicide islands, respectively. The top graphs show the details of the leftmost bar on the bottom graphs, and include data from both isolated nanowires and nanowires in bundles. Narrower widths shown by “A” come from the edges of bundled nanowires, and except for these data, there is no particular difference between the widths of bundled and isolated nanowires. For isolated nanowires, rectangular nanowires are wider than triangular ones. The most probable nanowire width is in the range in 2–3 nm, which corresponds to 5–9 silicide cells wide. The maximum nanowire width of ~ 5 nm can be related to the 6.8% lattice mismatch between HoSi_2 and Si substrate along the c axis. This was also noted for DySi_2 nanowires which have similar lattice mismatch and maximum width.⁴

The most probable nanowire height is 0.4–0.6 nm, which is 1–2 bulk HoSi_2 unit cell heights. Although we have statistics for comparatively few compact 3D islands, it is clear that both the width and the height of the compact silicide

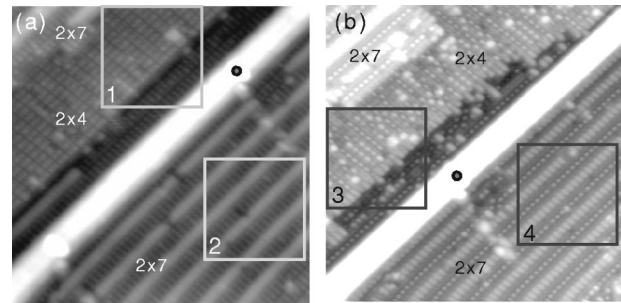


FIG. 7. (a) Empty- and (b) filled-state images of slightly different areas of the same surface with 0.55 ML Ho showing both 2×4 and 2×7 structures ($30 \times 30 \text{ nm}^2$). The position of gray circle on the nanowire in (a) corresponds to that in (b).

islands are spread over a much wider range than those for the nanowires. The fact that the 3D islands’ sizes can exceed the maximum width of the nanowires suggests that their growth is not coherent. It is possible that there are dislocations at the interface that do not propagate up to the surface of the islands. However, for most islands there is no clear indication of such dislocations from the STM images, unlike the dislocation networks observed for other epitaxial silicides grown on Si(111).⁷ Further work with transmission electron microscopy would be useful in clarifying the structure of the islands.

C. Two-dimensional substrate surface reconstructions

Figures 7(a) and 7(b) are empty- and filled-state images of slightly different areas of the same surface with 0.55 ML Ho. Coexistence of 2×4 and 2×7 structures on the 2D surface is observed. A nanowire runs diagonally across the image, and gray circles on both Figs. 7(a) and 7(b) indicate the same physical position on the surface.

Figures 8(a) and 8(b) show the empty-state (1.76 V) and filled-state (-1.76 V) images of the 2×4 structure corresponding to the square areas numbered by “1” and “3” in Fig. 7, respectively. These images are of the same area of the surface. Both figures have three sets of 2×4 unit cells along the Si dimer row direction ($[1\bar{1}0]$) outlined in white. In the empty-state image [Fig. 8(a)], three maxima are visible in each 2×4 unit cell. There are two types of maxima that are lined up in one of two possible configurations; a darker maximum (small circle) between brighter maxima (big circles), or a brighter maximum between two darker maxima. Either combination is equally probable. In the filled state image [Fig. 8(b)], the contrast between the two types of maxima is reversed, and more pronounced. Bright oval maxima appear in the positions of the darker filled state maxima.

By comparison of both bias images with respect to the Si(001) substrate, the registration of empty and filled state of maxima of the 2×4 structure can be diagrammed as in Fig. 8(c). All the empty-state maxima are positioned in what would normally be the centers of Si dimer positions, and the filled-state maxima are located in the same positions as the darker empty-state maxima. The overall character of the 2×4 structure is the same as that seen for Dy on Si(001).⁸

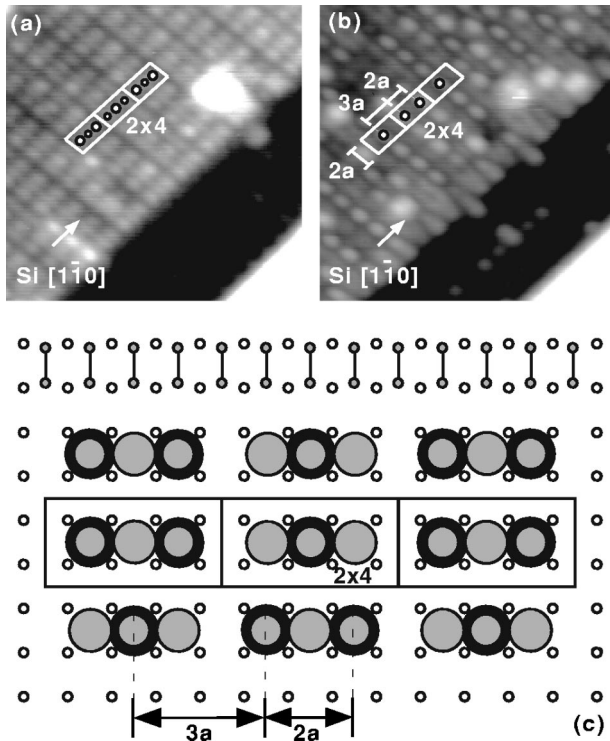


FIG. 8. (a) Empty-state (1.76 V) and (b) filled-state (-1.76 V) images of the 2×4 phase in the reconstructed surface shown in Fig. 7 ($10 \times 10 \text{ nm}^2$). (a) and (b) correspond to the square areas numbered by 1 and 3 in Fig. 7, respectively. (c) Line drawing showing the empty-state (gray circles) and filled-state (dark circles) maxima of the 2×4 structure. Clean 2×1 Si dimer positions are shown as a reference on the topmost low.

Figures 9(a) and 9(b) show enlargements of the 2×7 structure corresponding to the square areas numbered by “2” and “4” in Fig. 7, respectively. Two types of rows (rows A and B) are observed and three types of maxima are visible in both biases. In the empty-state image [Fig. 9(a)], row A consists of oblong maxima elongated along the $7 \times$ direction. Row B consists of three maxima and the smaller maximum is located between two larger maxima. In the filled-state image, row A includes paired maxima, and row B has three maxima and the larger maximum is located between two smaller maxima. The registration of 2×7 phase can be obtained by comparison with positions of 2×4 phase from both bias images.

The registration and approximate spatial extent of the empty- and filled-state maxima of the 2×7 structure are diagrammed in Fig. 9(c). This illustration contains five rows (row ABABA) which are seen in Fig. 9(b), and the clean 2×1 Si dimer row positions are shown on top as a reference. The empty-state maxima of the bright features in row A and B are represented by gray oblongs and circles, respectively. The filled-state maxima are illustrated using dark circles in three sizes. In row A, the paired filled-state of maxima are located on the bridge site, and an oblong empty-state maximum is positioned off bridge site. In row B, in both states, middle maximum is located on the bridge site, and the both edges of maxima are positioned off bridge site. Row A or B

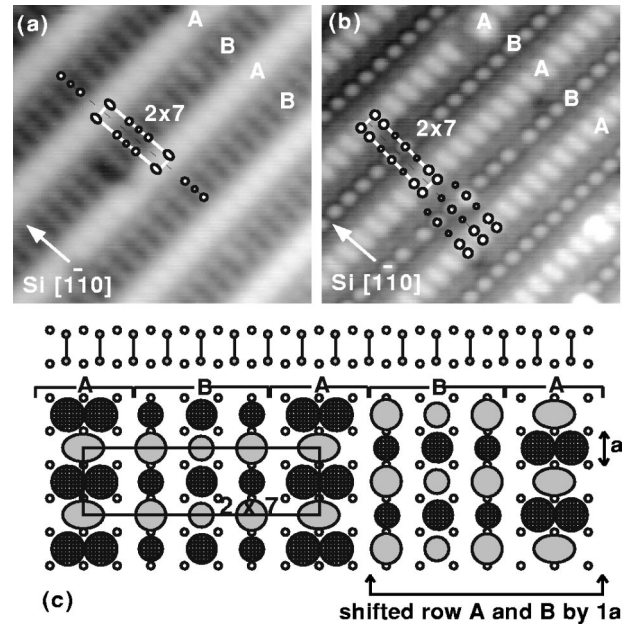


FIG. 9. (a) Empty-state (1.76 V) and (b) filled-state (-1.76 V) images of the 2×7 phase extracted from Fig. 7. (a) and (b) correspond to the square areas numbered by 2 and 4, respectively. A 2×7 unit cell consists of three types of maxima in rows labeled A and B in both images. (c) Line drawing showing the empty-state (gray circles and oblongs) and filled-state (dark circles) maxima of the 2×7 structure. 2×1 Si dimer positions from the clean surface are shown as a reference on the topmost low.

in both states often shifts by $1a$ in the perpendicular direction to the 2×1 Si dimer row ($[1\bar{1}0]$). In this sense, the overall periodicity should be defined as the coexistence of 2×7 and $c(2 \times 14)$ unit cells. For simplicity, we denote this phase by 2×7 . Since at a given coverage Ho metal can be distributed in nanowires and both the 2×4 and the 2×7 reconstructed surfaces, it is difficult to decide the density of Ho in the 2×7 structure. Therefore we are not proposing an atomic structure for the 2×7 phase.

D. Ho content of the 2×4 substrate reconstruction and the nanowires

From the results in Fig. 3, one can compare experimental coverage with calculated coverage under different assumptions for Ho content of both the 2D substrate reconstruction and the nanowires as shown in Fig. 10. The calculation was done on the basis of the first five coverages in Fig. 3. The table on the right in Fig. 10 shows two different assumptions of Ho content. The first assumption is the number of Ho atoms per 2×4 unit cell on the 2D surface: “A,” “B,” and “C” indicate one, one and half, and two Ho atoms per 2×4 unit cell, respectively. The second assumption is the number of metal layers in a nanowire: “1” and “2” represent one and two metal layers in the minimum height nanowire, respectively. Here we also assumed that each metal layer in the nanowire has a density of 1 ML as implied by the bulk crystal structure.⁴ The coverages shown in the graph on the

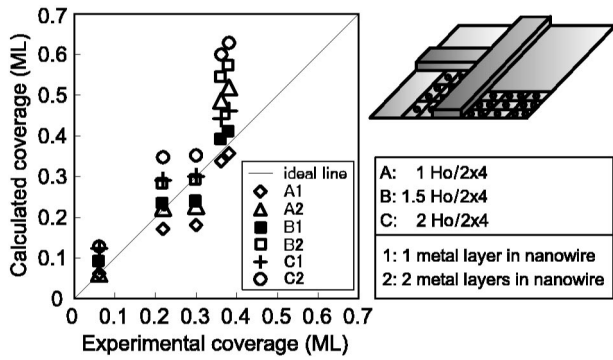


FIG. 10. Comparison of experimental coverage with calculated coverage under different assumptions of Ho content (see text)

left hand side where calculated under the six possible combinations of assumptions enumerated to the right, along with the measured percentage of the surface covered by bare surface, 2×4 , and nanowires as shown in Fig. 3. The best model should come closest to the diagonal line. Error bars are omitted for clarity. The error in coverage is less than 20%, and the error in the vertical position of the symbols is less than 10%.

As can be seen in the figure, the best fit is for B1 which implies 1.5 Ho atoms per 2×4 unit cell, and one layer of metal atoms in the minimum height nanowire. There is one layer of metal atoms in each bulk unit cell of the silicide, and so this is not a surprising result. Nevertheless, this coverage dependent analysis was necessary to deduce this fact since the geometric height of the first layer nanowires as seen by STM was bias dependent. We cannot exclude the possibility that the minimum height nanowire may have more than two layers of Si atoms, but this depends in some sense on the definition of where the substrate ends and the nanowire begins.

The 1.5 Ho atoms per 2×4 unit cell is somewhat more surprising. The simplest interpretation is that one of the two types of filled state maxima is associated with a single Ho atom. As shown in Fig. 8, two possible configurations of 2×4 unit cells alternate on the surface, one with a bright-dim-bright arrangement of maxima, and the other with a dim-bright-dim arrangement. There are equal populations of both types of unit cells, meaning that the average density of either type of maxima is 1.5 per 2×4 unit cell. This is not to say necessarily that the maxima seen in either bias is a Ho atom. In the case of the Dy 2×4 , there appears to be three metal atoms per unit cell and yet bright and dim maxima are seen as well. Determination of the atomic structure of the 2×4 surface and the origin of the differences between the Ho and Dy induced structures will require complementary information from other surface analytic techniques.

E. Scanning tunneling spectroscopy

Figure 11(a) shows the STS I - V curves and normalized spectra of a nanowire, 3D island, and the adjacent areas of reconstructed substrate at 0.56 ML. Since the 2D surface is reconstructed by Ho, the spectrum of the substrate is different from that of clean Si. The upper two curves are the actual

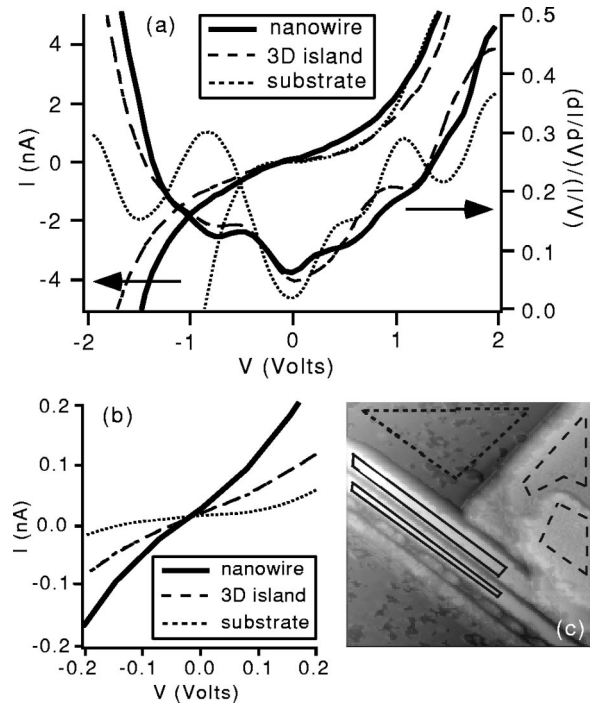


FIG. 11. (a) The STS I - V curves and normalized spectra for a nanowire, 3D island, and the reconstructed substrate. (b) Magnification of the STS I - V curves at near-zero bias voltage. Each STS spectrum was averaged from the STS data acquired in the areas shown by solid or dashed lines in the STM image shown in (c) ($40 \times 40 \text{ nm}^2$).

I - V data, and the lower three curves are the logarithmic derivative. STS data were acquired at every pixel of the image shown in Fig. 11(c). Each STS curve is an average of the data taken in the area enclosed by the solid or dashed lines. The normalized spectra show that the nanowire has nonzero conductivity at near-zero bias. Figure 11(b) is the STS I - V curves at near-zero bias voltage. It is clear that the I - V curve of the nanowire is steeper than that of 3D island and the reconstructed substrate. Although both nanowire and 3D island are metallic, nanowire has greater surface conductivity. Bulk HoSi_2 is metallic with a conductivity of approximate $4.4 \times 10^3 [(\Omega \text{ cm})]^{-1}$ at RT.⁹

IV. CONCLUSIONS

We have studied the initial stages of Ho growth on Si(001) surface. Metal coverages between 0.06–0.9 ML were deposited onto substrates heated to 600°C , and the samples were then cooled to room temperature for study by STM. Under these growth conditions, Ho forms either highly elongated silicide nanowires or compact 3D silicide islands, together with several possible Ho induced 2D substrate surface reconstructions. STS spectra reveal that the nanowires are more metallic than either the large 3D islands or the reconstructed substrate. The details of high coverage growth and preliminary transport measurements of a HoSi_2 nanowire network will be reported elsewhere.

- ¹J.A. Knapp and S.T. Picraux, *Appl. Phys. Lett.* **48**, 466 (1986).
- ²C. Preinesberger, S. Vandré, T. Kalka, and M. Dähne-Prietsch, *J. Phys. D* **31**, L43 (1998).
- ³Y. Chen, D.A.A. Ohlberg, G. Medeiros-Ribeiro, and Y.A. Chang, *Appl. Phys. Lett.* **76**, 4004 (2000).
- ⁴J. Nogami, B.Z. Liu, M.V. Katkov, and C. Ohbuchi, *Phys. Rev. B* **63**, 233305 (2001).
- ⁵O. Sakho, F. Sirotti, M. DeSantis, M. Sacchi, and G. Rossi, *Appl. Surf. Sci.* **56-58**, 568 (1992).
- ⁶D.J. Spence, S.P. Tear, T.C.Q. Noakes, and P. Bailey, *Phys. Rev. B* **61**, 5707 (2000).
- ⁷R. Stalder, H. Sirringhaus, N. Onda, and H. von Känel, *Appl. Phys. Lett.* **59**, 1960 (1991).
- ⁸B.Z. Liu and J. Nogami, *Surf. Sci.* **488**, 399 (2001).
- ⁹V.N. Eremenko, V.E. Listovnichii, S.P. Luzan, Y.I. Buyanov, and P.S. Martsenyuk, *J. Alloys Compd.* **219**, 181 (1995).